Directed assembly of optically bound matter

Michael D. Summers,[1] Richard D. Dear,[1] Jonathan M. Taylor,[2] and Grant A.D. Ritchie[1,*]

[1]*Department of Chemistry, PTCL, University of Oxford, South Parks Road, Oxford, OX1 3QZ, UK*
[2]*Department of Physics, Durham University, South Road, Durham DH1 3LE, UK*
[*]*grant.ritchie@chem.ox.ac.uk*

Abstract: We present a study of optically bound matter formation in a counter-propagating evanescent field, exploiting total internal reflection on a prism surface. Small ensembles of silica microspheres are assembled in a controlled manner using optical tweezers. The structures and dynamics of the resulting optically bound chains are interpreted using a simulation implementing generalized Lorentz-Mie theory. In particular, we observe enhancement of the scattering force along the propagation direction of the optically bound colloidal chains leading to a microscopic analogue of a driven pendulum which, at least superficially, resembles Newton's cradle.

OCIS codes: (240.0240) Optics at surfaces; (290.4020) Mie theory; (290.4210) Multiple scattering; (350.4855) Optical tweezers.

References and links

1. K. Dholakia and P. Zemánek, "Gripped by light: Optical binding," Rev. Mod. Phys. **82**(2), 1767–1791 (2010).
2. C. D. Mellor, J. Leckner, and C. D. Bain, "Pattern formation in evanescent wave optical traps," Proc. SPIE **5930**, 59301C, 59301C-10 (2005).
3. C. D. Mellor and C. D. Bain, "Array formation in evanescent waves," ChemPhysChem **7**(2), 329–332 (2006).
4. M. Šiler, M. Sery, T. Cizmar, and P. Zemanek, "Submicron particle localization using evanescent field," Proc. SPIE **5930**, 59300R, 59300R-9 (2005).
5. M. Šiler, T. Cizmar, M. Sery, and P. Zemanek, "Optical forces generated by evanescent standing waves and their usage for sub-micron particle delivery," Appl. Phys. B **84**(1-2), 157–165 (2006).
6. S. Kawata and T. Sugiura, "Movement of micrometer-sized particles in the evanescent field of a laser beam," Opt. Lett. **17**(11), 772–774 (1992).
7. M. Gu, J.-B. Haumonte, Y. Micheau, J. W. M. Chon, and X. Gan, "Laser trapping and manipulation under focused evanescent wave illumination," Appl. Phys. Lett. **84**(21), 4236 (2004).
8. C. D. Mellor, T. A. Fennerty, and C. D. Bain, "Polarization effects in optically bound particle arrays," Opt. Express **14**(21), 10079–10088 (2006).
9. P. J. Reece, V. Garcés-Chávez, and K. Dholakia, "Near-field optical micromanipulation with cavity enhanced evanescent waves," Appl. Phys. Lett. **88**(22), 221116 (2006).
10. V. Garcés-Chávez, R. Quidant, P. J. Reece, G. Badenes, L. Torner, and K. Dholakia, "Extended organization of colloidal microparticles by surface plasmon polariton excitation," Phys. Rev. B **73**(8), 085417 (2006).
11. M. D. Summers, R. D. Dear, J. M. Taylor, and G. A. D. Ritchie, "Controlled formation of optically bound matter in evanescent fields," Proc. SPIE **7762**, 776213, 776213-8 (2010).
12. N. J. van Leeuwen, L. J. Moore, W. D. Partridge, R. Peverall, G. A. D. Ritchie, and M. D. Summers, "Near-field optical trapping with an actively-locked cavity," J. Opt. **13**(4), 044007 (2011).
13. K. C. Neuman and S. M. Block, "Optical trapping," Rev. Sci. Instrum. **75**(9), 2787–2809 (2004).
14. M. M. Burns, J.-M. Fournier, and J. A. Golovchenko, "Optical binding," Phys. Rev. Lett. **63**(12), 1233–1236 (1989).
15. M. M. Burns, J.-M. Fournier, and J. A. Golovchenko, "Optical matter: crystallization and binding in intense optical fields," Science **249**(4970), 749–754 (1990).
16. S. A. Tatarkova, A. E. Carruthers, and K. Dholakia, "One-dimensional optically bound arrays of microscopic particles," Phys. Rev. Lett. **89**(28), 283901 (2002).
17. N. K. Metzger, K. Dholakia, and E. M. Wright, "Observation of bistability and hysteresis in optical binding of two dielectric spheres," Phys. Rev. Lett. **96**(6), 068102 (2006).
18. A. Constable, J. Kim, J. Mervis, F. Zarinetchi, and M. Prentiss, "Demonstration of a fiber-optical light-force trap," Opt. Lett. **18**(21), 1867–1869 (1993).
19. M. Guillon, O. Moine, and B. Stout, "Longitudinal optical binding of high optical contrast microdroplets in air," Phys. Rev. Lett. **96**(14), 143902 (2006).

#155364 - $15.00 USD Received 26 Sep 2011; revised 15 Nov 2011; accepted 2 Dec 2011; published 4 Jan 2012

20. V. Garcés-Chávez, D. Roskey, M. D. Summers, H. Melville, D. McGloin, E. M. Wright, and K. Dholakia, "Optical Levitation in a Bessel Light Beam," Appl. Phys. Lett. **85**(18), 4001 (2004).
21. V. Karásek, O. Brzobohaty, and P. Zemanek, "Longitudinal optical binding of several spherical particles studied by the coupled dipole method," J. Opt. A, Pure Appl. Opt. **11**(3), 034009 (2009).
22. J. M. Taylor and G. D. Love, "Optical binding mechanisms: a conceptual model for Gaussian beam traps," Opt. Express **17**(17), 15381–15389 (2009).
23. P. C. Chaumet and M. Nieto-Vesperinas, "Optical binding of particles with or without the presence of a flat dielectric surface," Phys. Rev. B **64**(3), 035422 (2001).
24. Y. L. Xu and B. A. S. Gustafson, "Comparison between multisphere light-scattering calculations: rigorous solution and discrete-dipole approximation," Astrophys. J. **513**(2), 894–909 (1999).
25. J. M. Taylor, L. Y. Wong, C. D. Bain, and G. D. Love, "Emergent properties in optically bound matter," Opt. Express **16**(10), 6921–6929 (2008).
26. J. P. Barton, D. R. Alexander, and S. A. Schaub, "Theoretical determination of net radiation force and torque for a spherical particle illuminated by a focused laser beam," J. Appl. Phys. **66**(10), 4594–4602 (1989).
27. D. W. Mackowski, "Analysis of radiative scattering for multiple sphere configurations," Proc. R. Soc. Lond. A **433**(1889), 599–614 (1991).
28. H. Chew, D.-S. Wang, and M. Kerker, "Elastic scattering of evanescent electromagnetic waves," Appl. Opt. **18**(15), 2679–2687 (1979).
29. E. E. M. Khaled, S. C. Hill, and P. W. Barber, "Scattered and internal intensity of a sphere illuminated with a Gaussian beam," IEEE Trans. Antenn. Propag. **41**(3), 295–303 (1993).
30. J. A. Stratton, *Electromagnetic Theory* (McGraw-Hill, 1941).
31. S. Chang, J. H. Jo, and S. S. Lee, "Theoretical calculations of optical force exerted on a dielectric sphere in the evanescent field generated with a totally-reflected focused Gaussian beam," Opt. Commun. **108**(1-3), 133–143 (1994).
32. G. Videen, "Light scattering from a sphere on or near a surface," J. Opt. Soc. Am. A **8**(3), 483–489 (1991).
33. D. W. Mackowski, "Exact solution for the scattering and absorption properties of sphere clusters on a plane surface," J. Quant. Spectrosc. Radiat. Transf. **109**(5), 770–788 (2008).
34. M. Abramowitz and I. A. Stegun, *Handbook of mathematical functions* (Dover, 1972).
35. P. Zemanek, A. Jonas, P. Jakl, J. Jezek, M. Sery, and M. Liska, "Theoretical comparison of optical traps created by standing wave and single beam," Opt. Commun. **220**(4-6), 401–412 (2003).
36. J. Lekner, "Force on a scatterer in counter-propagating coherent beams," J. Opt. A, Pure Appl. Opt. **7**(5), 238–248 (2005).
37. V. Karásek, T. Cizmár, O. Brzobohatý, P. Zemánek, V. Garcés-Chávez, and K. Dholakia, "Long-range one-dimensional longitudinal optical binding," Phys. Rev. Lett. **101**(14), 143601 (2008).

1. Introduction

There have been a number of recent studies involving the trapping of multiple particles using evanescent waves formed at interfaces by counter-propagating laser beams, as comprehensively reviewed by Dholakia and Zemánek [1]. The spatial distributions adopted by the particles are determined both by the underlying optical potential associated with the interference fringes and the interparticle light scattering, while the relative contribution of each effect in determining these "optically bound" structures are a sensitive function of the particle size parameter, x (= $2\pi\ a/\lambda$ where a is the radius of the particle and λ is the wavelength of the trapping radiation). The first observations of one-dimensional optical binding in evanescent wave systems were reported by Mellor and Bain [2, 3], and Siler *et al.* [4, 5] in 2005. These studies built upon earlier work by Kawata and Sugiura [6], where colloidal particles were confined on the surface of a prism using counter-propagating beams incident at an angle just above the critical angle. The optical gradient provided by the resulting evanescent fields caused particles near the surface to accumulate in the region of highest light intensity [7]. Interestingly, experiments using sub-μm diameter particles resulted in the formation of close-packed 2-d crystals, strongly influenced by both interference fringes produced by the counter-propagating coherent beams and coherent scattering between multiple particles [8]. Similar experiments conducted by Reece *et al*. enhanced the optical forces using resonant dielectric waveguides [9] and surface plasmon resonance techniques [10]. Alternatively the evanescent field intensity can be enhanced by placing the interface within an actively locked optical cavity [11, 12].

While optical tweezing forces are well understood [13], interactions in multiple particle systems are less so. The origin of these binding forces was first described in 1989 in the work of Burns *et al*. [14], examining the forces induced by an optical field between two dielectric

#155364 - $15.00 USD Received 26 Sep 2011; revised 15 Nov 2011; accepted 2 Dec 2011; published 4 Jan 2012

spheres, and was later extended to studies of colloidal crystals illuminated by multiple optical standing waves [15]. The term "optically bound matter" was used to describe the structures formed by dielectric colloidal particles in the presence of applied optical fields. Subsequently optical binding effects have been observed in other experiments [16–18] dealing with dielectric particles in counter-propagating light fields and in experiments using only a single levitating beam [19] as well as with different beam geometries, such as Bessel beams [20].

A number of theoretical models have been used to explore these optical binding effects. These include the coupled dipole method [21] and Generalized Lorenz-Mie Theory (GLMT) [22], both of which use the same underlying vector wave treatment of light. The coupled dipole method is a volume discretization method more easily applied to arbitrarily-shaped bodies and complex light beams [23], but one which can suffer from subtle convergence issues [24]; GLMT is arguably more analytically complex but is computationally more efficient, which can be a crucial advantage, particularly for studies of dynamics. Such models typically deal with small ensembles of particles due to the complex nature of multiple scattering processes. Recent experiments [25] have shown that, for large chains of particles, multiple scattering effects become increasingly important relative to the background optical potential. There is still much work to be done to bridge the gap between these simple model systems and the more complex structures observed in reality, and our aim in this paper is to further explore the transition between these two regimes using a simple counter-propagating evanescent trap in combination with optical tweezers [12]. The controlled assembly of one-dimensional chains using the optical tweezers allows us to explore the interparticle interactions and develop a corresponding implementation of GLMT which is capable of predicting both static and dynamic properties of this optically bound matter.

2. Experimental method

The experiment is constructed around a modified Leica microscope as shown in Fig. 1. A 1064 nm solid state laser (Crystalaser) is collimated and aligned into the back aperture of the imaging objective (Leica Hi-Plan, 100× NA = 1.2) using a 4*f* imaging system. The tweezers position can therefore be controlled using the single mirror located in the conjugate plane. The optical power to the tweezers can be controlled using a half-wave plate and polarizing beam splitter placed before the steering optics. Precise *z*-axis placement of the tweezers spot in the focal plane of the microscope can be adjusted a small amount using lenses L1 and L2 in the 4*f* system, with focal lengths of 100 and 200 mm respectively, before causing noticeable off-axis aberration of the tweezers. A truncated isosceles fused silica prism is mounted with the top surface in the focal plane of the objective lens. White light illumination is provided from below the prism by the microscope light source, allowing samples on the top surface to be imaged onto a CCD using the same microscope objective [12].

The evanescent component of the trap is built around the silica glass isosceles prism (n = 1.45) cut to an angle of 68° (θ_c = 66.7°). The output from a Laser Quantum Forte system (maximum power of 400 mW at 1064 nm) is coupled into a polarization maintaining fiber-splitter to produce two output beams of equal intensity which are focused onto the prism from opposing directions using 50 mm lenses held in *x*-*y*-*z* adjustable mounts. The exact experimental conditions used are as follows: two coherent counter-propagating spots with a major radius of 20 μm and a separation of 50 μm; an angle of incidence of 1.3° greater than the critical angle; a peak intensity contribution of 0.48 mW μm^{-2} on the surface from each fiber; and p-polarization used in both propagation directions (controlled by half-wave plates). Sample chambers are prepared using thickness #1 coverslips and thin polyvinyl spacers, which allow the focal plane of the tweezers to lie on the prism surface. The samples are pipetted directly onto the prism surface and the sample chamber placed on top. The samples themselves consist of 3.5 μm diameter silica spheres (Bangs Laboratories SS05N) suspended in Milli-Q water (Millipore) in concentrations optimized to avoid clutter in the region of interest. Typical sample lifetimes are on the order of 1 hour.

#155364 - $15.00 USD Received 26 Sep 2011; revised 15 Nov 2011; accepted 2 Dec 2011; published 4 Jan 2012

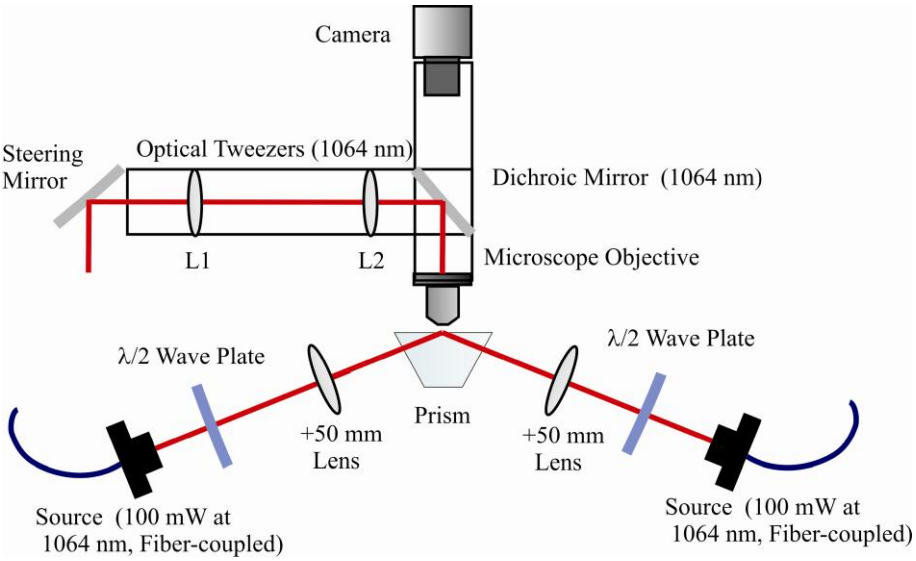

Fig. 1. The experimental setup. The apparatus is divided into 2 parts. Both the evanescent optical trap and the optical tweezers are built into a commercial microscope (Leica). A CrystaLaser (350 mW at 1064 nm, but with typically only 10 mW used in the tweezer itself) is focused by a 100× NA = 1.2 microscope objective (Leica) onto the prism surface. The resulting tweezers are controlled manually by manipulation of the steering mirror. A Laser Quantum Forte laser is coupled into a polarization maintaining optical fiber splitter, producing 100 mW at 1064 nm of light in each output arm. The two mutually coherent beams are then focused onto the prism surface at an angle greater than the critical angle of the prism. Polarization is controlled using the half-wave plates in each arm. Imaging of the trapped samples is done through the microscope objective and recorded on a CCD (Watec 902-H3).

3. GLMT simulation of evanescent optical binding

Our experimental system is simulated using an exact vector description of coherent monochromatic light. This optical model can be applied to particles of any size, but is most efficient for Mie particles i.e. of dimensions comparable to the wavelength of the light. Our approach is broadly similar to that used in previous work [25], including theoretical work by other authors to include considerations such as optical forces acting on particles [26] and multiple particle interactions [27]. In addition, important roles are played by two factors that are not normally considered in GLMT calculations; these are the effects of scattered light reflected by the prism surface and the focused nature of the illuminating Gaussian beams. Both of these effects are now detailed below.

3.1 Gaussian evanescent wave

To our knowledge, there is very little published work that takes full account of the Gaussian profile of the laser beam used to produce the evanescent trapping field by total internal reflection (TIR). In the case of an extremely broad laser spot, such effects can be ignored and the beam can be approximated as an ideal evanescent wave (using the formulation used previously in [25] and derived in [28]). If the laser is more tightly focused the particles will be exposed to different evanescent field strengths depending on their position on the prism surface. Such a scenario can still be modeled using the standard beam shape coefficients for an ideal evanescent wave, but with the intensity that any given particle is exposed to being determined by its position in the field. In such a scheme the local field around the particle is still modeled as that of an ideal evanescent wave. While this model is an improvement it still cannot, for example, represent gradient force effects drawing particles towards the center of the laser beam spot. A more rigorous approach considers the incoming Gaussian beam in

#155364 - $15.00 USD Received 26 Sep 2011; revised 15 Nov 2011; accepted 2 Dec 2011; published 4 Jan 2012

terms of its plane wave spectrum. Each individual plane wave is treated separately in its interaction with the interface; depending on the angle of incidence of that plane wave component, the wave may merely be refracted at the interface or may undergo TIR, producing an evanescent wave on the far side of the interface. When all these components are recombined, the correct representation of the field on the far side of the interface in response to the incident beam is obtained.

Our simulation uses the plane wave decomposition method of Khaled *et al*. [29], calculating the interaction of each wave vector with the interface [30] and representing the components using standard evanescent or plane wave expansions as appropriate. This is similar to the approach used by Chang *et al*. [31], except for our retention of non-evanescent components of the incident beams which can have a measurable effect when the angle of incidence is close to the critical angle. This approach gives a good representation of a paraxial Gaussian beam, although naturally the plane wave decomposition of the beam breaks down for very high numerical apertures. In our case, the beam waist is of the order of 10 μm and the paraxial approximation is quite valid.

3.2 Surface reflections

When a particle scatters light from the evanescent field, the resultant outgoing wave impinges upon the substrate and the wave may be reflected. These reflections may then impinge upon other particles, including the original particle, modifying the field around them and hence the optical force acting on the system. Unfortunately, a planar interface such as our prism surface does not fit well with the spherical symmetry of the basis functions used in GLMT. Although a perfectly reflecting surface can be treated in terms of image sources, and for a single particle the approximation of normal incidence may sometimes be reasonable [32, 33], the general case of reflection by a dielectric surface is an extremely challenging problem that often requires numerical solution of integrals to determine the matrix coefficients for the basis-set transformation. To this end we have implemented a scheme based on the equations derived by Mackowski [33]. One detail of the implementation worth noting relates to the Jacobi polynomials $P_n^{(\alpha,\beta)}$, which appear in the reflection integrals and must be evaluated for relatively large, negative values of α. This is a situation in which standard recursive or iterative evaluation methods [34] suffer from catastrophic cancellation when implemented using standard double-precision arithmetic. The solution to this is to factorize the relevant Jacobi polynomials once at the start of the simulation (using extended precision arithmetic). Subsequent to this, a polynomial can be efficiently evaluated as a product of its factors using double-precision arithmetic.

To highlight the importance of surface reflections in our system, Fig. 2 plots the optical forces between two spheres, both of diameter 3.5 μm and resting on the substrate, as a function of their separation for a number of different calculation methods. Firstly, the force is shown without taking into account any reflections from the substrate, and also with a full reflection calculation. It can be readily seen that the inclusion of surface reflections can significantly alter the inter-particle separation at which the optical force between the particles is zero. Secondly, an approximation is shown where the planar substrate is replaced by a large sphere with the same properties as the substrate. This approximation, not described elsewhere in the literature to our knowledge, was very useful for quickly estimating the significance or otherwise of surface reflections. The same (exact) background evanescent field is still used, but surface reflections are approximated using the appropriate GLMT multiple reflection coefficients for the large sphere used as a proxy for the substrate. In our case it established that surface reflections are important and prompted the implementation of the full, rigorous calculation. It also provides an independent verification of the correctness of the full reflection model implementation, with surprisingly good agreement between the full reflection calculation and the approximation.

#155364 - $15.00 USD Received 26 Sep 2011; revised 15 Nov 2011; accepted 2 Dec 2011; published 4 Jan 2012

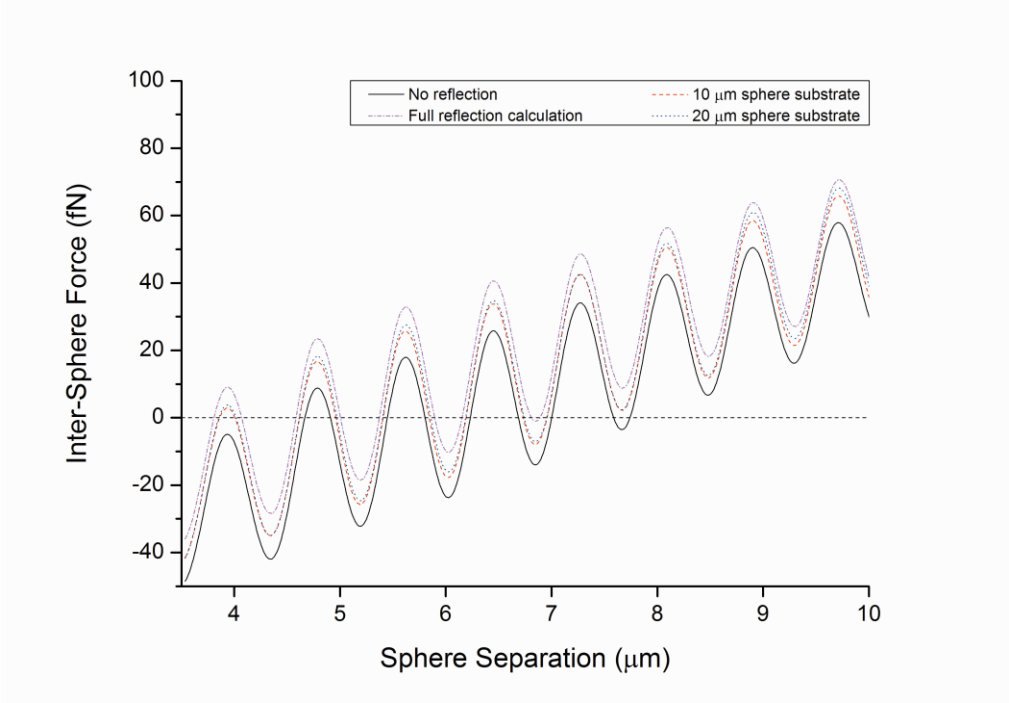

Fig. 2. The optical force between two 3.5 μm diameter spheres resting on the substrate as a function of inter-sphere spacing. Forces are shown with and without substrate reflections taken into account, and results are also shown for an alternative, approximate method of handling surface reflections that uses a large dielectric spherical surface as an approximation to the planar surface.

4. Results and discussion

4.1 Particle equilibrium conditions

In order to examine optical binding effects as closely as possible and to facilitate a comparison with our GLMT model, we used the tweezers to assemble linear chains of 3.5 μm diameter silica microspheres in the evanescent field on the prism surface. This particle size was selected due to the weak interaction of the particles with the underlying optical potential [35, 36] ensuring that scattering/binding forces are principally responsible for determining the resultant structures.

Figure 3 shows a typical example of the controlled formation of optically bound chains as individual particles are added sequentially, clearly showing that the average separation between the particles decreases as the number of particles in the chain increases. In this case we observe *"chain collapse"* when a 5^{th} particle is added to the chain; this corresponds to a phase transition towards a configuration where the particles are almost in physical contact [37]. This chain collapse is a general phenomenon and is commonly observed when a 5^{th} particle is added, however we note that in some cases the collapse does not occur until the addition of a 6^{th} particle. Chain collapse on addition of the 5^{th} particle is evident in Fig. 4a, which shows values of the interparticle separation for a single example run, averaged over 30 seconds. Before making comparisons with theory we note firstly that the interparticle separation is not constant within the chain but is largest between the end particles and their nearest neighbours in the chain; similar effects have been observed and modeled in counterpropagating fibre traps [22]. Secondly, for a given number of particles in the chain, the optically bound structures can access a wide range of sizes. For example, Fig. 4b shows the spread of particle separations observed for two particles over a period of one minute as they

#155364 - $15.00 USD Received 26 Sep 2011; revised 15 Nov 2011; accepted 2 Dec 2011; published 4 Jan 2012

move about an average value of 8.6 μm with a standard deviation of 1.2 μm. Thirdly, as the optical forces present in our experiment are far weaker than those acting on particles in, for example, optical tweezers traps (tens of fN compared to pN) we must consider the role of electrostatic repulsion between the colloidal particles in determining the optically bound structures. We have conducted studies using both ultra pure Milli-Q water and a range of samples with $NaNO_3$ concentrations of up to 0.5 mM; in the former low screening case the Debye length is on the order of 1 μm while for the most highly charge-screened sample used the Debye length is 14 nm. In general we find that increased screening leads to a modest decrease in the average chain length for a fixed particle number but that this change is generally smaller than the variation in the chain lengths that are observable both within a single run due to the Brownian motion of the particles within the chain, and between repeated measurement on different samples. We therefore conclude that electrostatics do not play an important role in determining the structures of the observed optically bound matter.

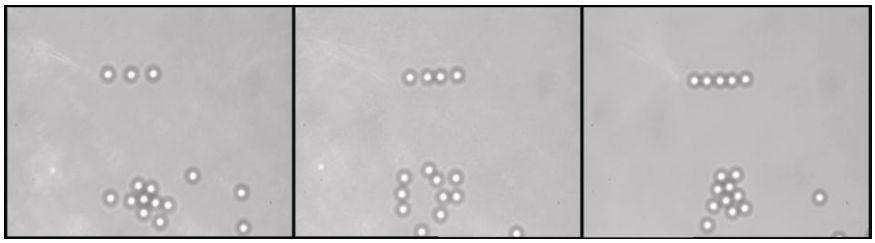

Fig. 3. Controlled assembly of a chain of 3.5 μm silica microspheres in an evanescent field (top half of each image). Particles are moved from the pool of loose particles (bottom half of each image) using optical tweezers. The chain is observed to fill the optical potential, collapsing in the centre when a 5th particle enters the chain. Each screenshot is taken approximately 1 minute after the addition of a new particle to allow the chain equilibrium positions to be reached.

The resulting force plots from our simulations provide equilibrium chain lengths, and examples of these are shown in Fig. 5; the intercepts of each curve with the *x*-axis show points at which the net force acting on the outermost particles in the chain equals zero, and those intercepts with positive-gradient intersections represent stable positions. For the larger chains, the number of degrees of freedom make it difficult to fully explore the full parameter space in this rather challenging calculation. As a result of this we have applied a number of restrictions to our simulations. For these examples of stable chains we have assumed symmetry about the centre of the chain. For the 4-particle plot shown here, the spacing between the central two particles was allowed to reach equilibrium as well, but for 5 and 6 particles we have assumed the central particles to be in contact with each other (minimum possible spacing). The positive compressive force on these central particles (not shown in the figure) confirms that such a chain configuration as a whole is stable. Thus the results obtained from simulation are fully stable configurations, but we note that other stable configurations with reduced symmetry may also be possible.

#155364 - $15.00 USD Received 26 Sep 2011; revised 15 Nov 2011; accepted 2 Dec 2011; published 4 Jan 2012

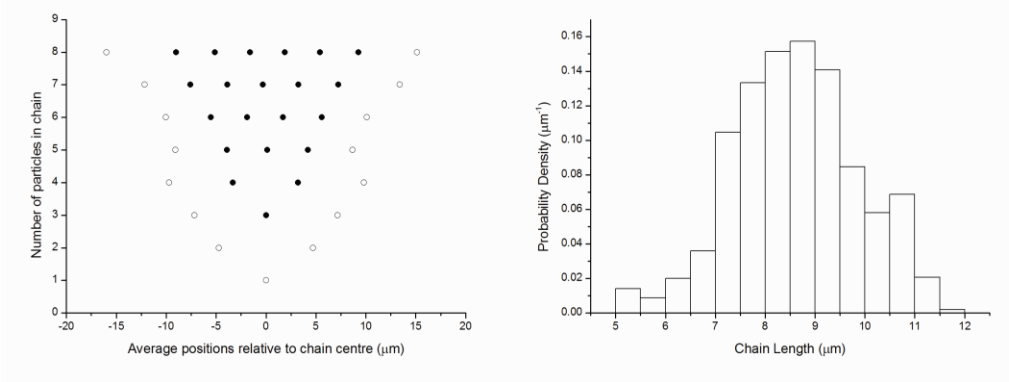

Fig. 4. a (Left) Average particle positions for an example experimental run as a function of the number of particles in the chain. Positions are averaged over 30 seconds and clearly show both the "chain collapse" at 5 particles as the particles in the chain come into contact, and the decrease in interparticle separation observed towards the chain centre for a given chain length. b (Right) The probability density of interparticle separation for the case of 2 particles. The variation in length of a chain of two particles is taken over a period of one minute and shows a standard deviation of 1.2 μm.

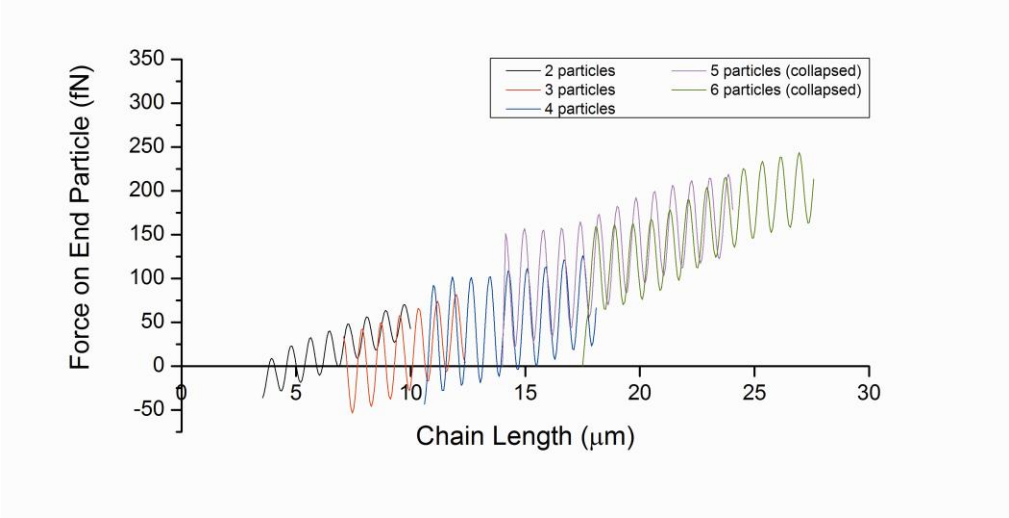

Fig. 5. A typical output plot using our evanescent wave optical binding simulation, in the absence of charge effects. In this plot, where compressive forces are shown as positive, stable chains are indicated by positive-gradient intersections of each curve with the x-axis. The full conditions on the central particles are indicated in the text. The interplay between optical forces and scattering effects acting on the spheres in small linear chains leads to complete coalescence of the chain with the addition of a 5th particle, to form a chain where all particles are in contact.

These results indicate that there are multiple stable chain configurations for a given number of particles. Our simulation results report the largest stable chain lengths, since we expect these to be the kinetic product in experiments where chains are built up by addition of further particles at initially large distances from the trap centre. At the laser intensities used, the particles have a low probability of crossing the potential barriers required to access the smaller equilibrium interparticle spacings. In order to compare our experimental and theoretical results, we have calculated the average chain separations from several sets of experiments. For example, for a system of two particles, we observe average chain lengths ranging from 6.4 – 9.3 μm from different runs with standard deviations of around 1μm for each run. In Fig. 6 we have plotted the average of these values, with the error bars being the

#155364 - $15.00 USD Received 26 Sep 2011; revised 15 Nov 2011; accepted 2 Dec 2011; published 4 Jan 2012

standard deviation from a single representative run. We see good qualitative agreement between experiment and theory for 2, 3 and 4 particles, with a divergence at 5 particles due to the simulation predicting complete chain collapse at this point while the experiment often requires a 6th particle to initiate collapse. We have also included data from a single example run where collapse at 5 particles was observed, which shows closer agreement with the simulation. It is clear that the chains very rarely collapse such that the particles are truly in physical contact.

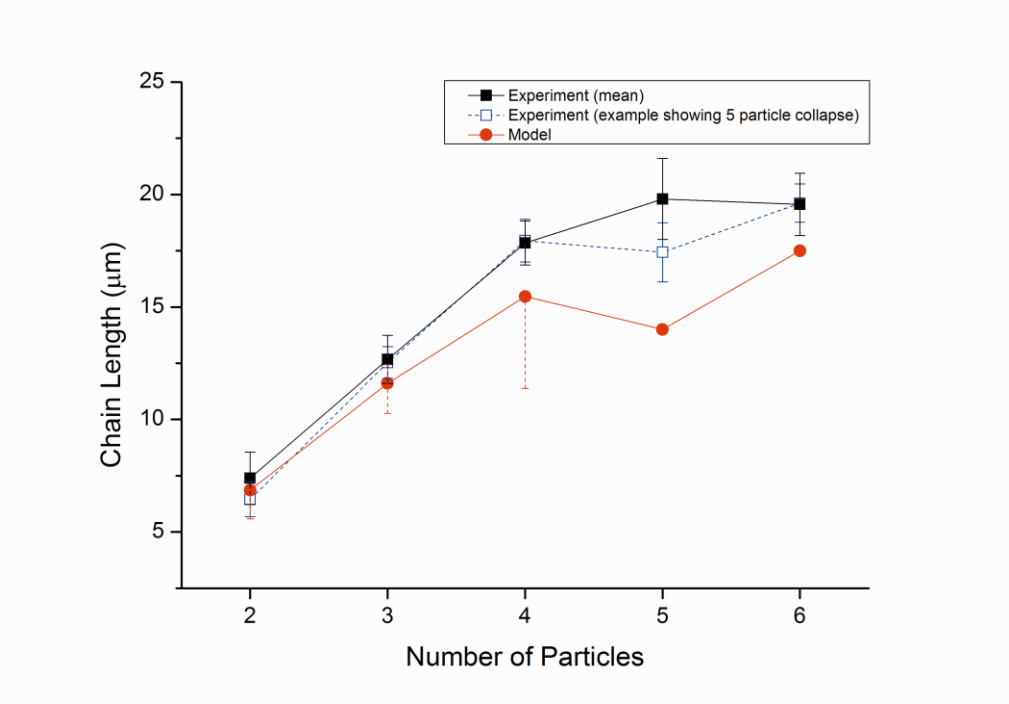

Fig. 6. Plot comparing simulated equilibrium chain lengths and experimental results for charge screened samples. The experimental points are the average of several runs with the error bars representing the standard deviation observed within a single typical run. Since the experimental datapoints are averages between multiple experimental runs, the point at 5 particles includes some chains which have collapsed, and some which have not. As such, the results diverge from the simulation which predicts complete collapse at this point. An example of an experimental run which does demonstrate collapse at 5 particles has also been included for comparison. Uncertainty in the simulation parameters is estimated on the basis of a potential 5% uncertainty in the sphere radii and illuminating spot radii, 1% in the refractive index of the spheres and 0.2% in the angle of incidence of the beam.

4.2 Particle dynamics

During our studies we also observe emergent dynamic behaviour in longer chains such as chain collapse, tilting and off-axis drift [25]. Perhaps the most striking dynamical effect observed was what we have dubbed “Newton’s Cradle” motion, in which particles are ejected from the ends of chains with velocity components both in and out of the plane of the interface; at a certain height and distance from the optically bound chain the free particle then rejoins the chain under the influence of both gravity and optical binding/scattering forces. Media 1 shows this process occurring over a 2 minute interval, playing at 8x speed, with screenshots given in Fig. 7. This emergent behaviour was only observable under experimental conditions that used the highest intensities available.

#155364 - $15.00 USD Received 26 Sep 2011; revised 15 Nov 2011; accepted 2 Dec 2011; published 4 Jan 2012

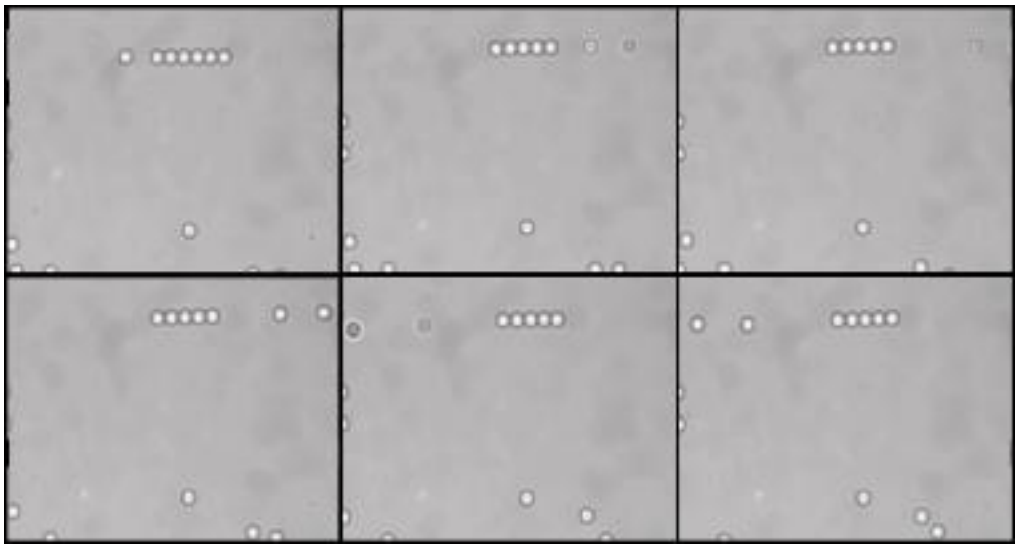

Fig. 7. Screenshots of the "Newton's Cradle" motion from above from top left to bottom right taken from Media 1. A particle is allowed to drift in from the left hand side into a linear chain of 6 particles. The two right-most particles are ejected out of the plane (moving out of focus) due to the force due to the scattered light being guided along the chain being greater than that provided by the evanescent field. The particles then fall back into the evanescent field due to gravity and are pushed back into the chain, repeating the process on the other side. The period of oscillation is approximately 2 minutes in this example, with the video playing at 8x speed.

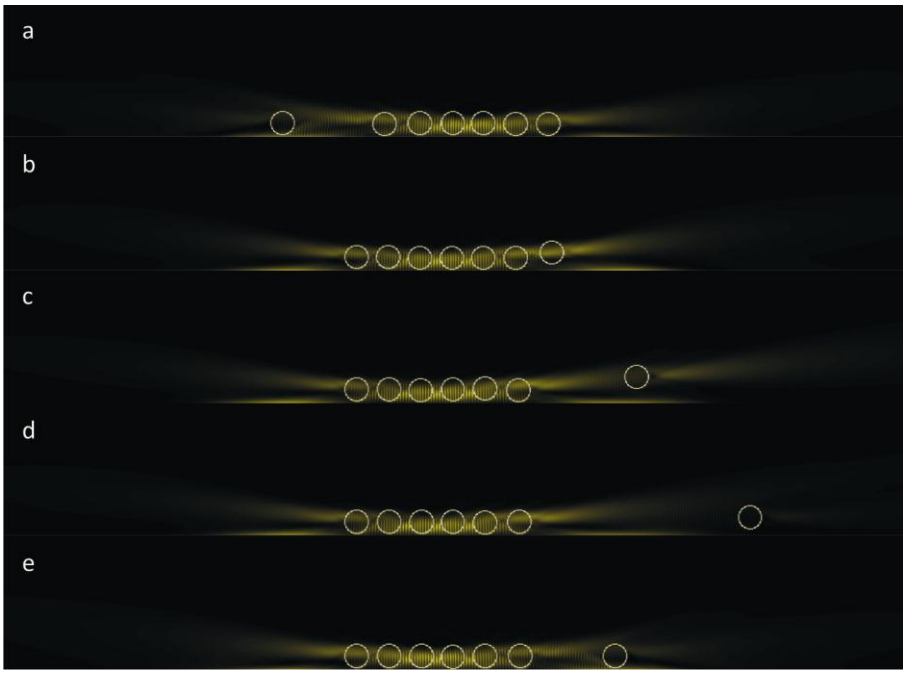

Fig. 8. Simulation screenshots of "Newton's Cradle" motion (side view) with the light intensity marked in yellow. The particles are ejected out of the plane in agreement with experiment.

The complex, non-linear dynamics of this driven system are qualitatively predicted by our simulations, and these are shown in Fig. 8. We have already noted the difficulties in dealing with larger chains of particles and the increased number of degrees of freedom, and therefore

#155364 - $15.00 USD Received 26 Sep 2011; revised 15 Nov 2011; accepted 2 Dec 2011; published 4 Jan 2012

the simulations presented here are restricted in that they consider particle Brownian motion but ignore the effects of surface reflections. The simulations predict a period of oscillation a factor of four smaller than we observe experimentally, perhaps due to the treatment of scattered light and the ejection of a single particle rather than the two ejected experimentally. Despite these differences, the simulation does however offer real insight into the physical processes which govern the chain dynamics as we now explain.

The refractive index contrast between the microspheres and the surrounding water results in two closely coupled phenomena: frustrated total internal reflection, and "waveguiding" effects, both of which can be seen in Fig. 8. As a sphere approaches from the left and passes over the left-hand laser focus (a) it causes an additional beam of light to escape through the prism and illuminate the chain of spheres. This radiation is then waveguided through the optically bound chain structure and is sufficiently intense to draw the rightmost sphere away from the prism surface (b). Once this has occurred, the horizontal and vertical restoring force exerted on it by the right-hand laser focus is dramatically reduced due to its evanescent decay with height, while the waveguiding effect ensures that the influence of the left-hand laser on it continues. This lack of a restoring force means that the particle can be ejected from the end of the chain and away from the trapping region (c). After travelling some distance this particle then falls under the influence of gravity (d), returning to the substrate surface where it is drawn back into the trapping region (e), thus perpetuating the circulatory process and resulting in the effect reminiscent of a "Newton's cradle" toy.

Critical to this effect is the presence of the intensity-modulated fringes caused by interference between the two counter-propagating laser beams. These provide a potential barrier that individual spheres must cross in order to move along the substrate surface. If the intensity is too great then particles will require a strong additional force to cross the fringes, while at low intensities particles are largely unaffected by their presence. At an intermediate intensity the fringes are able to introduce hysteresis into the system in terms of the horizontal position of the particles, an effect aided by small vertical displacements of particles within the chain which experience a reduced evanescent field. This hysteresis appears to be a key element of the "Newton's cradle" effect, enabling regular periodic motion in this overdamped system.

We also note that under the same experimental conditions there exist trajectories for which particles can be ejected from the chain back in the direction from which they have just arrived. This has also been observed in numerical simulations, and the direction in which particles are ejected appears to be extremely sensitive to the exact experimental conditions, as well as the instantaneous configuration of particles within the chain.

5. Conclusion

We have explored the dynamics of 1-dimensional chains of optically bound matter in evanescent fields by combining optical tweezers with an evanescent trap utilizing total internal reflection at the surface of a prism. Both equilibrium and dynamic effects have been investigated under conditions in which the scattering forces are relatively strong compared to the contribution of the evanescent interference fringes typically characteristic of such systems. These studies were used to assist in the development of a simulation of light scattering in evanescent fields using Generalized Lorentz-Mie Theory (GLMT). Our theoretical model agrees with the observed results for short particle chains sufficiently well in order to explain the compression of chains with particle number due to the modified light field, as well as dynamic effects caused by coherent light scattering between multiple particles in such an ensemble.

With a working model of the behavior of optically bound matter in evanescent fields, we will investigate more complex systems and a range of particles of varying morphology and composition. The hybrid tweezers/evanescent trapping geometry developed here will also

#155364 - $15.00 USD Received 26 Sep 2011; revised 15 Nov 2011; accepted 2 Dec 2011; published 4 Jan 2012

allow mapping of forces in the evanescent field and the exploration of optical effects peculiar to a total internal reflection geometry, such as the Goos-Hänchen shift.

Acknowledgments

MDS and RD would like to thank the Leverhulme Trust and the EPSRC for the award of a postdoctoral research fellowship and a postgraduate studentship respectively.

#155364 - $15.00 USD Received 26 Sep 2011; revised 15 Nov 2011; accepted 2 Dec 2011; published 4 Jan 2012